

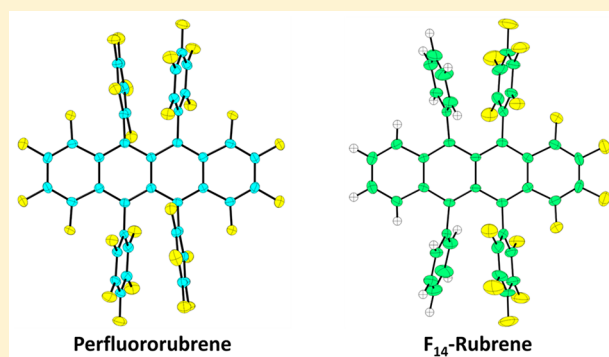
Perfluorinated and Half-Fluorinated Rubrenes: Synthesis and Crystal Packing Arrangements

Youichi Sakamoto and Toshiyasu Suzuki*

Institute for Molecular Science, Myodaiji, Okazaki 444-8787, Japan

S Supporting Information

ABSTRACT: Perfluororubrene (PF-RUB) has been synthesized by cycloaddition of perfluorinated 1,3-diphenylisobenzofuran and 1,4-diphenyl-2,3-didehydronaphthalene followed by reductive deoxygenation. This method was easily applied for the synthesis of half-fluorinated rubrene (F_{14} -RUB). The electrochemical measurements and DFT calculations indicate that perfluorination strongly lowers the HOMO and LUMO energies. Recrystallization and sublimation of PF-RUB gave two different crystals with planar and twisted conformations, respectively. In both cases, perfluorination leads to the formation of short C–F and F–F contacts and completely disrupts face-to-face π interactions. Single crystals of F_{14} -RUB were grown by sublimation, and twisted molecules display the two-dimensional π -stacking with a face-to-face distance of 3.54 Å.



INTRODUCTION

Rubrene (RUB) is a unique tetracene derivative that has bulky phenyl substituents at the 5, 6, 11, and 12 positions (Chart 1). RUB crystallizes in a herringbone motif and forms one-dimensional (1D) π -stacking along its long molecular axis.¹ This is quite different from the herringbone packing of the parent tetracene, which shows two-dimensional (2D) edge-to-face interactions.² Because of this unusual crystal structure, single-crystal field-effect transistors of RUB showed remarkably high hole mobility as p-type organic semiconductors.^{3,4} This steric approach has often been applied for other tetracene and pentacene derivatives to realize 1D slipped π -stack and 2D brick packing arrangements.⁵

Perfluorination is a simple method to prepare an n-type semiconductor with the same molecular symmetry.⁶ It is interesting to see how perfluorination keeps or changes a packing motif of RUB. Collaborating with Schreiber and co-workers, we have already reported the physical properties of perfluororubrene (PF-RUB) and half-fluorinated rubrene (F_{14} -RUB) (Chart 1) in comparison with RUB.^{7–10} In the meantime, Douglas and co-workers reported a synthetic route for PF-RUB, which is based on sequential addition of (perfluorophenyl)lithium to perfluorotetracenequinone (7% total yield over six steps).¹¹ Very recently, they prepared partially fluorinated rubrenes (Scheme S1, Supporting Information), including 5,6,11,12-tetrakis(perfluorophenyl)-tetracene (F_{20} -RUB) and 5,12-bis(perfluorophenyl)-6,11-diphenyltetracene (F_{10} -RUB).¹² A systematic study of the crystal structures showed that C–F...X (X = H, F, and π) intermolecular interactions play a major role in determining molecular conformation and crystal packing. In this paper, we

report the syntheses and crystal structures of two fluorinated rubrenes, PF-RUB and F_{14} -RUB. Electrochemical measurements and DFT calculations were also performed to understand the impact of perfluorination on the electronic properties and crystal structures of RUB.

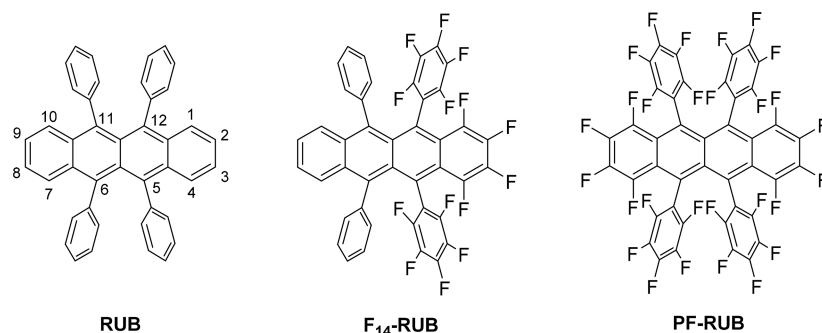
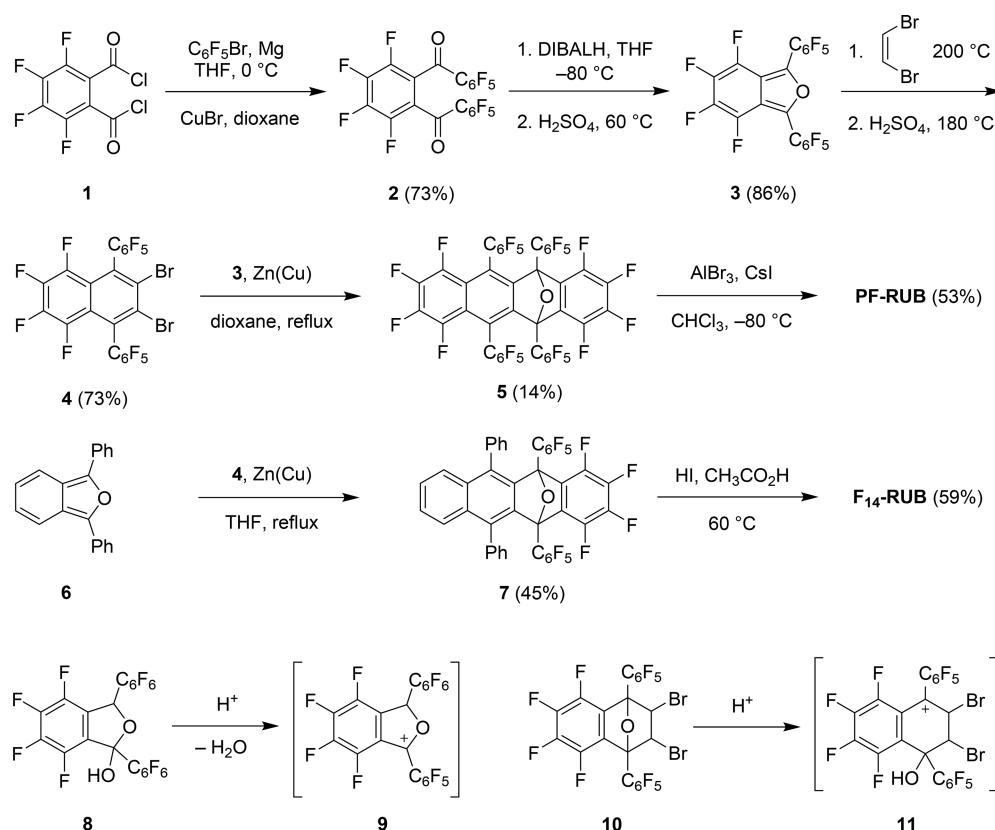
RESULTS AND DISCUSSION

For the synthesis of symmetrically and unsymmetrically fluorinated rubrenes, we modified the naphthyne (didehydronaphthalene) cycloaddition approach.¹³ In this route, 1,3-diarylisobenzofurans¹⁴ such as **3** and **6** are key intermediates. As shown in Scheme 1, (perfluorophenyl)copper, prepared from (perfluorophenyl)magnesium bromide¹⁵ and copper(I) bromide, was allowed to react with perfluorophthaloyl dichloride¹⁶ (**1**) to afford perfluoro-1,2-dibenzoylbenzene (**2**). Reduction of **2** with DIBALH followed by acid-catalyzed dehydration of lactol **8** gave perfluoro-1,3-diphenylisobenzofuran (**3**). Usually, trifluoroacetic acid is efficient for dehydration of lactols.¹⁷ However, we needed to use concd H_2SO_4 because cation **9** is destabilized by electronegative fluorine atoms. Cycloaddition of **3** with 1,2-dibromoethylene was carried out in a sealed tube at 200 °C. Apparently, **3** was less reactive as a diene compared to 1,3-diphenylisobenzofuran (**6**). Oxo-bridged adduct **10** was then heated at 180 °C in concd H_2SO_4 for dehydration to yield perfluoro-2,3-dibromo-1,4-diphenylnaphthalene (**4**). The harsh conditions were required due to the destabilization of cation **11** by fluorine atoms. Treatment of dibromide **4** with *n*-butyllithium resulted in a byproduct which

Received: June 4, 2017

Published: July 6, 2017

Chart 1. Structures of Rubrene, Half-Fluorinated Rubrene, and Perfluorinated Rubrene

Scheme 1. Synthesis of PF-RUB and F₁₄-RUB

did not react with **3**. We examined various reagents to generate the 2,3-naphthylene in situ and found that a zinc–copper couple could give the adduct **5** in low yield. Cesium iodide in the presence of aluminum tribromide¹³ reduced oxo-bridged compound **5** to provide PF-RUB. Similarly, cycloaddition of **6** and **4** with the zinc–copper couple afforded oxo-bridged adduct **7** in moderate yield. Reduction of **7** with HI in acetic acid gave half-fluorinated rubrene, F₁₄-RUB. The total yields of PF-RUB and F₁₄-RUB from **1** are 3% and 12%, respectively.

PF-RUB and F₁₄-RUB were purified by temperature gradient sublimation. They are red crystalline solids similar to RUB. UV–vis absorption and fluorescence spectra have already been discussed in our previous paper (Figure S1, Supporting Information).⁷ Cyclic voltammograms (CVs) were also reported by Anger et al.¹⁰ and Zhang et al.¹¹ recently (Figure S2a, Supporting Information). Differential pulse voltammograms (DPVs) displayed more redox peaks than CVs (Figure S2b). PF-RUB showed one oxidation and two reduction peaks

(Table 1). The first oxidation and reduction potentials shifted positively by more than 1 V compared to those of RUB. This

Table 1. Redox Potentials^a (V) of Rubrene Compounds by Differential Pulse Voltammetry

compd	E _{ox,2}	E _{ox,1}	E _{red,1}	E _{red,2}	ΔE (E _{ox,1} – E _{red,1})
PF-RUB		1.56	–0.92	–1.60	2.48
F ₁₄ -RUB	1.42	0.96	–1.48	–2.06	2.44
RUB	0.98	0.36	–2.06		2.42

^aVersus Fc/Fc⁺, scan rate 20 mV/s, 0.1 M (n-Bu)₄NPF₆ in 1,2-dichloroethane.

indicates that perfluorination strongly lowers the HOMO and LUMO energies.

DFT calculations were performed with the B3LYP (Table S2, Supporting Information), M06-L (Table S3, Supporting Information), and ωB97XD (Table S4, Supporting Information) functionals and the 6-31G(d,p) basis set. Optimized

geometries of PF-RUB and F₁₄-RUB are twisted as reported for RUB and its derivatives (Figure S3, Supporting Information).^{12,18,19} The planar conformations were also calculated to evaluate the planarization energies: $\Delta E = E(\text{planar}) - E(\text{twisted})$ (Table S1, Supporting Information). Unlike previous rubrene derivatives,^{12,18} the planarization energy of PF-RUB (6.7 kcal mol⁻¹ by B3LYP) is much larger than that of RUB (3.7 kcal mol⁻¹). In a PF-RUB molecule, two perfluorophenyl groups at the 5 and 6 (and 11 and 12) positions get close to each other by the steric effect of two fluorine atoms at the 4 and 7 (and 1 and 10) positions, which increases the steric repulsion between the two aryl groups. This is probably more effective in the planar backbone. Similarly, the aryl intercentroid distances of PF-RUB and F₁₄-RUB are shorter than that of RUB, even though the twist angles are larger in the fluorinated rubrenes (Table 2). As observed in the

Table 2. DFT Data of Optimized Geometries Calculated at the B3LYP/6-31G(d,p) Level

compd	twist angle ^a (deg)	intercentroid distance (Å)	HOMO energy (eV)	LUMO energy (eV)	gap (eV)
PF-RUB	53.1 [50.6] ^b	3.54 [3.26] ^b	-6.09	-3.69	2.40
F ₁₄ -RUB	48.4 [42.1] ^b	3.57 [3.29] ^b	-5.37	-2.93	2.44
RUB	42.0 [41.1] ^b	3.71 [3.54] ^b	-4.63	-2.12	2.51

^aDihedral angle between C2–C3 and C8–C9. ^bCalculated at the M06-L/6-31G(d,p) level.

DPVs, perfluorination lowers the HOMO and LUMO energies by more than 1 eV. In contrast, the HOMO–LUMO gaps do not change so much, which is also in agreement with the ΔE values in the DPVs (Table 1).

Single crystals of PF-RUB were grown by recrystallization or sublimation and analyzed by X-ray diffraction. We obtained two different crystal structures, one with a planar conformation (monoclinic, *P2₁/c*)^{20,21} from CH₂Cl₂/EtOH (Figure 1a) and another with a twisted conformation (monoclinic, *P2₁/n*)²² by

sublimation (Figure 2a). The end-to-end twist angle of a tetracene backbone is 45.9°. As shown in Figures 1b and 2b, both planar and twisted PF-RUB crystals lose π – π interactions, which is important for carrier mobility. We only found short C–F and F–F contacts (less than the sum of the van der Waals radii) between the tetracene cores. Interestingly, a single crystal of planar PF-RUB ($V/Z = 843.0 \text{ \AA}^3$) is denser than that of twisted PF-RUB ($V/Z = 891.0 \text{ \AA}^3$). The larger intermolecular interactions might stabilize less stable planar backbones. Anger et al. obtained IR and Raman spectra of polycrystalline PF-RUB films on SiO₂ and observed both planar and twisted structures.⁹ They proposed on the basis of their annealing experiment that the crystal structure with planar PF-RUB molecules would be thermodynamically more stable because of its efficient packing. Indeed, a planar PF-RUB molecule displays many C–F and F–F short contacts with 14 neighboring molecules mainly via perfluorophenyl–perfluorophenyl and perfluorophenyl–tetracene interactions (Figure S5, Supporting Information). Sutton et al. suggested that perfluorination would increase these intermolecular interactions as well as the intramolecular interaction between the two aryl groups by electrostatic and dispersion forces.¹⁸

In the case of 5,12-bis(4-fluorophenyl)-6,11-diphenyltetracene (F₂-RUB),¹⁹ its single crystal is isostructural (orthorhombic, *Cmca*) with that of RUB (Figure S4, Supporting Information). The cell volume only increased by 1.3% ($V/Z = 689.0 \text{ \AA}^3$ for RUB and 698.3 \AA^3 for F₂-RUB). Because PF-RUB is heavily fluorinated, the cell volumes for planar and twisted PF-RUB crystals increase by 22.3% and 29.3%, respectively. It is interesting to see how the packing motif of PF-RUB changes when fluorination is reduced by half.

Single crystals of F₁₄-RUB were grown by sublimation (orthorhombic, *Pnna*). The cell volume ($V/Z = 805.5 \text{ \AA}^3$) increases by 16.9% relative to that of RUB.²³ Although the tetracene backbone is twisted with an angle of 38.6° (Figure 3a), π – π interactions are seen between the tetracene cores. As shown in Figure 3b, fluorinated (C₆F₄) and nonfluorinated

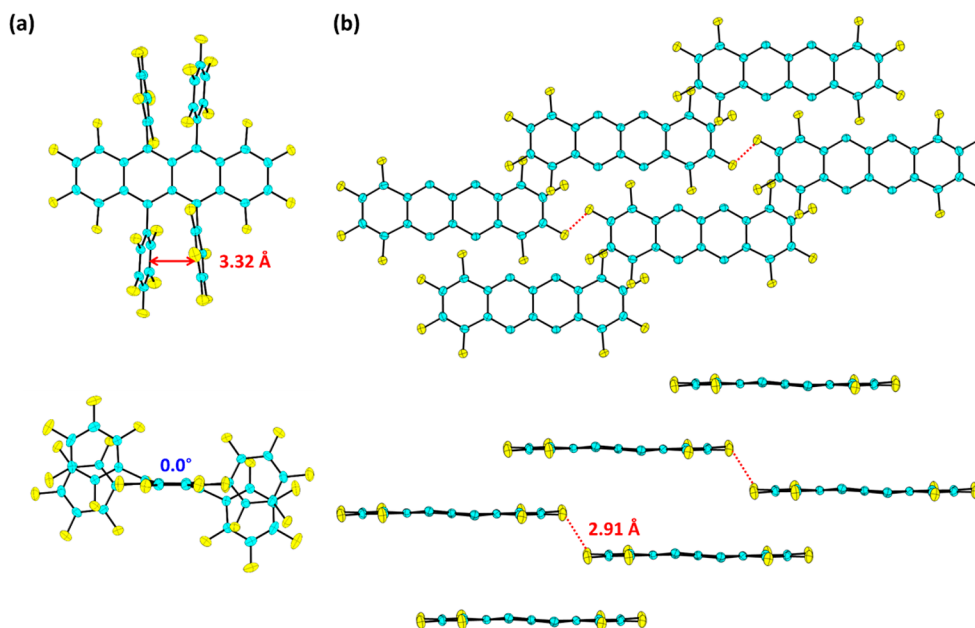


Figure 1. (a) Planar conformation of PF-RUB in a single crystal grown from solution. The intercentroid distance is shown. (b) Crystal packing of PF-RUB (planar). Only tetracene cores are shown for clarity. Dotted lines indicate short F–F contacts.

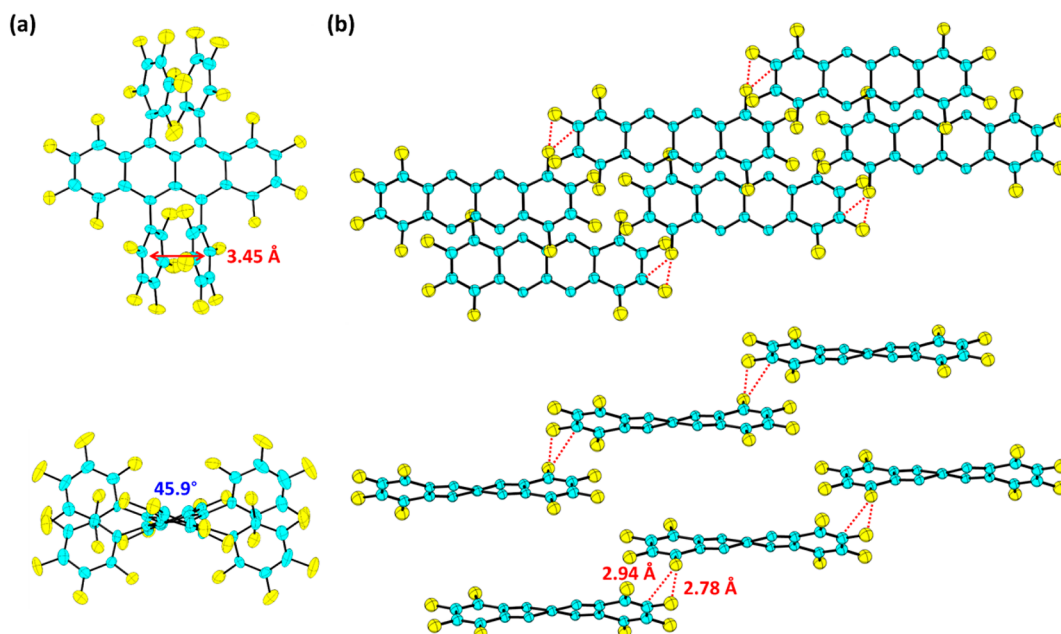


Figure 2. (a) Twisted conformation of PF-RUB in a single crystal grown by sublimation. The intercentroid distance and twist angle are shown. (b) Crystal packing of PF-RUB (twisted). Only tetracene cores are shown for clarity. Dotted lines indicate short C–F and F–F contacts.

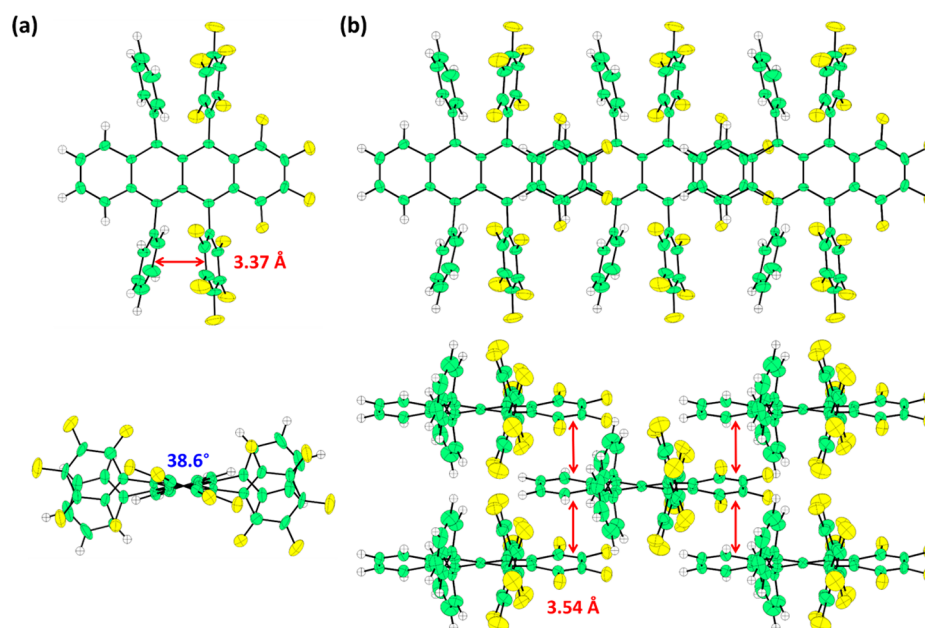


Figure 3. (a) Twisted conformation of F_{14} -RUB in a single crystal grown by sublimation. The intercentroid distance and twist angle are shown. (b) 2D π -stacking of F_{14} -RUB. Arrows indicate intermolecular π - π interactions.

(C_6H_4) rings of the tetracene backbone face each other with an interplanar distance of 3.54 Å. This arene–perfluoroarene interaction²⁴ has also been found in partially fluorinated tetracene and pentacene derivatives.^{25,26} An F_{14} -RUB molecule interacts with four neighboring enantiomers, which forms a 2D π network.⁵ This is in contrast with the 1D π -stacking of RUB molecules in a herringbone motif (Figure S4b). Interestingly, F_{14} -RUB molecules in a 2D layer are aligned in the same direction,²⁷ even though F_{14} -RUB has a large dipole moment.⁷ This orientation was also found in the second layer of F_{14} -RUB thin films deposited on Au(111) and Ag(111).⁸

In conclusion, we showed another route for PF-RUB, which can be easily applied for the synthesis of F_{14} -RUB. Perfluoro-

1,3-diphenylisobenzofuran (**3**) will be a useful synthetic building block to produce various fluorinated acenes.²⁸ F_{14} -RUB will be a good candidate for ambipolar single-crystal field-effect transistors because of its 2D brick packing.

EXPERIMENTAL SECTION

General Experimental Methods. All reactions were carried out under an argon atmosphere unless aqueous solutions were used. 1H and ^{19}F chemical shifts were referenced to internal tetramethylsilane and hexafluorobenzene ($\delta = 0.0$ ppm), respectively. In ^{13}C NMR, most of the signals were not detected due to multiple ^{13}C – ^{19}F couplings. Flash chromatographic separations were performed using a Yamazen Hi-Flash column (silica gel, 40 μm). Anhydrous copper(I) bromide was dried at 120 °C for 2 h under reduced pressure before use.

1,2-Bis(perfluorobenzoyl)-3,4,5,6-tetrafluorobenzene (2). A solution of bromopentafluorobenzene (48.6 g, 196 mmol) in THF (200 mL) was added dropwise to magnesium turnings (4.69 g, 193 mmol) in THF (100 mL) at 0 °C. The mixture was stirred at room temperature for 1 h. Anhydrous copper(I) bromide (55.3 g, 386 mmol) was added to the resulting dark brown solution, and the mixture was stirred at room temperature for 1 h. After addition of dioxane (100 mL), the resulting gray suspension was stirred at room temperature for 1 h. Perfluorophthaloyl dichloride¹⁶ (**1**; 24.1 g, 87.6 mmol) was added to the suspension at 0 °C, and the mixture was stirred at 0 °C for 30 min and at room temperature overnight. The resulting suspension was filtered through Celite, washed with CHCl₃, and evaporated under reduced pressure. The residue was dissolved in CHCl₃, and the solution was passed through silica gel. After removal of the solvent, the residue was recrystallized from CHCl₃/*n*-hexane to give **2** (34.4 g, 73%): mp 121–122 °C; ¹⁹F NMR (470 MHz, CDCl₃) δ 24.4 (d, *J* = 14.0 Hz, 2F), 21.7 (td, *J* = 19.9, 5.8 Hz, 4F), 17.1 (tt, *J* = 21.0, 5.8 Hz, 2F), 16.2 (d, *J* = 14.0 Hz, 2F), 2.47–2.64 (m, 4F); HRMS (EI/quadrupole) *m/z* calcd for C₂₀F₁₄O₂ [M⁺] 537.9675, found 537.9666.

4,5,6,7-Tetrafluoro-1,3-bis(perfluorophenyl)isobenzofuran (3). Diisobutylaluminum hydride (62 mL of a 1.03 M solution in hexane, 64 mmol) was added dropwise to a mixture of **2** (29.5 g, 54.8 mmol) in THF (200 mL) at –80 °C. The reaction mixture was stirred at room temperature for 2 h, poured into 1 M H₂SO₄ (200 mL), and extracted with ether. The extract was washed with brine, dried over Na₂SO₄, and concentrated under reduced pressure. After concentrated H₂SO₄ (30 mL) was added to the residue, the mixture was stirred at 60 °C for 30 min and poured onto crushed ice. The resulting solid was collected by filtration and washed with water. The crude product was recrystallized from EtOH to give **3** (24.6 g, 86%): mp 113–115 °C; ¹⁹F NMR (470 MHz, CDCl₃) δ 23.1–23.3 (m, 4F), 12.7 (t, *J* = 21.0 Hz, 2F), 11.6–11.8 (m, 2F), 6.53–6.63 (m, 2F), 1.40–1.59 (m, 4F); HRMS (EI/quadrupole) *m/z* calcd for C₂₀F₁₄O [M⁺] 521.9726, found 521.9719.

2,3-Dibromo-5,6,7,8-tetrafluoro-1,4-bis(perfluorophenyl)naphthalene (4). In a sealed glass tube, a mixture of **3** (23.5 g, 45.0 mmol) and 1,2-dibromoethylene (25.0 g, 135 mmol) was heated at 200 °C overnight. After removal of an excess of 1,2-dibromoethylene, the residue was chromatographed on silica gel with hexane to give the adduct **10**. A mixture of **10** and concentrated H₂SO₄ (200 mL) was stirred at 180 °C for 6 h, cooled to room temperature, and poured onto crushed ice. The resulting solid was collected by filtration and washed with water. The crude product was recrystallized from EtOH to give **4** (22.6 g, 73%): mp 196–197 °C; ¹⁹F NMR (470 MHz, CDCl₃) δ 21.7 (dd, *J* = 21.0, 5.8 Hz, 4F), 20.6–20.7 (m, 2F), 10.6–10.7 (m, 2F), 10.1 (t, *J* = 21.0 Hz, 2F), 0.77 (td, *J* = 21.0, 5.8 Hz, 4F); HRMS (EI/quadrupole) *m/z* calcd for C₂₂Br₂F₁₄ [M⁺] 689.8123, found 689.8141.

1,2,3,4,7,8,9,10-Octafluoro-5,12-dihydro-5,12-epoxy-5,6,11,12-tetrakis(perfluorophenyl)tetracene (5). A mixture of **3** (574 mg, 1.10 mmol), **4** (690 mg, 1.00 mmol), and a zinc–copper couple (85.0 mg, 1.30 mmol) in dioxane (10 mL) was refluxed for 5 days. The reaction mixture was diluted with toluene, filtered through Celite, and washed with toluene. After removal of the solvent, addition of *n*-hexane to the residue followed by filtration gave **5** (143 mg, 14%): mp 305–307 °C; ¹⁹F NMR (470 MHz, CDCl₃) δ 34.4–34.6 (m, 2F), 27.9–28.3 (m, 2F), 26.4–26.6 (m, 2F), 24.3–24.5 (m, 2F), 23.9–24.2 (m, 2F), 18.7 (d, *J* = 15.6 Hz, 2F), 14.8 (t, *J* = 21.4 Hz, 2F), 12.4 (t, *J* = 21.4 Hz, 2F), 11.9 (d, *J* = 14.8 Hz, 2F), 10.6 (d, *J* = 15.6 Hz, 2F), 3.12 (td, *J* = 21.4, 7.40 Hz, 2F), 2.25 (td, *J* = 21.4, 8.23 Hz, 2F), 1.46 (td, *J* = 21.4, 8.23 Hz, 2F), 0.09 (td, *J* = 21.4, 7.40 Hz, 2F); HRMS (EI/quadrupole) *m/z* calcd for C₄₂F₂₈O [M⁺] 1051.9502, found 1051.9484.

1,2,3,4,7,8,9,10-Octafluoro-5,6,11,12-tetrakis(perfluorophenyl)tetracene (PF-RUB). AlBr₃ (1.1 mL of a 1.0 M solution in dibromomethane, 1.1 mmol) was added dropwise to a mixture of **5** (564 mg, 0.536 mmol) and cesium iodide (577 mg, 2.22 mmol) in CHCl₃ (10 mL) at –80 °C. The reaction mixture was stirred at room temperature for 3 days and poured into an aqueous solution of sodium

metabisulfite. The organic layer was separated, dried over Na₂SO₄, and concentrated under reduced pressure. The resulting red solid was recrystallized from CH₂Cl₂/EtOH to give PF-RUB (295 mg, 53%): mp 288–289 °C; ¹⁹F NMR (470 MHz, CDCl₃) δ 24.9 (dd, *J* = 21.0, 5.8 Hz, 8F), 19.6–19.7 (m, 4F), 12.2–12.3 (m, 4F), 11.9 (t, *J* = 21.0 Hz, 4F), 0.48 (td, *J* = 21.0, 5.8 Hz, 8F); HRMS (EI/quadrupole) *m/z* calcd for C₄₂F₂₈ [M⁺] 1035.9553, found 1035.9545.

1,2,3,4-Tetrafluoro-5,12-bis(perfluorophenyl)-6,11-dihydro-6,11-diphenyl-6,11-epoxytetracene (7). A mixture of 1,3-diphenylisobenzofuran (**6**, 2.46 g, 9.10 mmol), **4** (5.71 g, 8.28 mmol), and a zinc–copper couple (650 mg, 9.94 mmol) in THF (20 mL) was refluxed for 2 days. The reaction mixture was diluted with CHCl₃, filtered through Celite, and washed with CHCl₃. After removal of the solvent, the residue was chromatographed on silica gel with *n*-hexane/CHCl₃ to give **7** (3.00 g, 45%): mp 230–233 °C; ¹⁹F NMR (470 MHz, CDCl₃) δ 25.6 (d, *J* = 23.9 Hz, 2F), 23.4 (d, *J* = 23.9 Hz, 2F), 18.5 (d, *J* = 16.5 Hz, 2F), 7.88 (t, *J* = 21.4 Hz, 2F), 7.19 (d, *J* = 16.5 Hz, 2F), –1.34–1.14 (m, 4F); ¹H NMR (500 MHz, CDCl₃) δ 7.86–7.92 (m, 2H), 7.73–7.80 (m, 4H), 7.30–7.38 (m, 8H); HRMS (EI/quadrupole) *m/z* calcd for C₄₂H₁₄F₁₄O [M⁺] 800.0821, found 800.0814.

1,2,3,4-Tetrafluoro-5,12-bis(perfluorophenyl)-6,11-diphenyltetracene (F₁₄-RUB). A mixture of **7** (1.29 g, 1.61 mmol), 55% aqueous HI (5 mL), 50% aqueous H₃PO₂ (0.5 mL), and acetic acid (20 mL) was stirred at 60 °C overnight. After the reaction mixture was poured into an aqueous solution of sodium metabisulfite, the resulting red solid was collected by filtration, washed with water, and recrystallized from CH₂Cl₂/EtOH to give F₁₄-RUB (744 mg, 59%): mp 331–332 °C; ¹⁹F NMR (470 MHz, CDCl₃) δ 24.5 (dd, *J* = 21.5, 7.2 Hz, 4F), 18.8–18.9 (m, 2F), 7.65 (t, *J* = 21.5 Hz, 2F), 6.20–6.30 (m, 2F), –2.46 (td, *J* = 21.5, 7.2 Hz, 4F); ¹H NMR (500 MHz, CDCl₃) δ 7.27–7.41 (m, 10H), 7.09 (d, *J* = 7.08 Hz, 4H); HRMS (EI/quadrupole) *m/z* calcd for C₄₂H₁₄F₁₄ [M⁺] 784.0872, found 784.0865.

■ ASSOCIATED CONTENT

Supporting Information

The Supporting Information is available free of charge on the ACS Publications website at DOI: 10.1021/acs.joc.7b01383.

Crystallographic data for PF-RUB (planar) (CIF)

Crystallographic data for PF-RUB (twisted) (CIF)

Crystallographic data for F₁₄-RUB (CIF)

UV–vis absorption and fluorescence spectra, cyclic and differential pulse voltammograms, crystal packing diagrams, computational details, energies and coordinates for the calculated compounds, and ¹H and ¹⁹F NMR spectra (PDF)

■ AUTHOR INFORMATION

Corresponding Author

*E-mail: toshy@ims.ac.jp

ORCID

Toshiyasu Suzuki: 0000-0003-4572-2384

Notes

The authors declare no competing financial interest.

■ ACKNOWLEDGMENTS

The computations were performed using the Research Center for Computational Science, Okazaki, Japan. We thank the Institute for Molecular Science for financial support.

■ REFERENCES

(1) Jurchescu, O. D.; Meetsma, A.; Palstra, T. T. M. *Acta Crystallogr., Sect. B: Struct. Sci.* **2006**, *62*, 330.

- (2) Holmes, D.; Kumaraswamy, S.; Matzger, A. J.; Vollhardt, K. P. C. *Chem. - Eur. J.* **1999**, *5*, 3399.
- (3) Sundar, V. C.; Zaumseil, J.; Podzorov, V.; Menard, E.; Willett, R. L.; Someya, T.; Gershenson, M. E.; Rogers, J. A. *Science* **2004**, *303*, 1644.
- (4) Takeya, J.; Yamagishi, M.; Tominari, Y.; Hirahara, R.; Nakazawa, Y.; Nishikawa, T.; Kawase, T.; Shimoda, T.; Ogawa, S. *Appl. Phys. Lett.* **2007**, *90*, 102120.
- (5) Anthony, J. E. *Chem. Rev.* **2006**, *106*, 5028.
- (6) Sakamoto, Y.; Suzuki, T.; Kobayashi, M.; Gao, Y.; Fukai, Y.; Inoue, Y.; Sato, F.; Tokito, S. *J. Am. Chem. Soc.* **2004**, *126*, 8138.
- (7) Anger, F.; Scholz, R.; Adamski, E.; Broch, K.; Gerlach, A.; Sakamoto, Y.; Suzuki, T.; Schreiber, F. *Appl. Phys. Lett.* **2013**, *102*, 013308.
- (8) Anger, F.; Glowatzki, H.; Franco-Cañellas, A.; Bürker, C.; Gerlach, A.; Scholz, R.; Sakamoto, Y.; Suzuki, T.; Koch, N.; Schreiber, F. *J. Phys. Chem. C* **2015**, *119*, 6769.
- (9) Anger, F.; Scholz, R.; Gerlach, A.; Schreiber, F. *J. Chem. Phys.* **2015**, *142*, 224703.
- (10) Anger, F.; Breuer, T.; Ruff, A.; Klues, M.; Gerlach, A.; Scholz, R.; Ludwigs, S.; Witte, G.; Schreiber, F. *J. Phys. Chem. C* **2016**, *120*, 5515.
- (11) Zhang, Z. R.; Ogden, W. A.; Young, V. G.; Douglas, C. J. *Chem. Commun.* **2016**, *52*, 8127.
- (12) Ogden, W. A.; Ghosh, S.; Bruzek, M. J.; McGarry, K. A.; Balhorn, L.; Young, V.; Purvis, L. J.; Wegwerth, S. E.; Zhang, Z. R.; Serratore, N. A.; Cramer, C. J.; Gagliardi, L.; Douglas, C. J. *Cryst. Growth Des.* **2017**, *17*, 643.
- (13) Dodge, J. A.; Bain, J. D.; Chamberlin, A. R. *J. Org. Chem.* **1990**, *55*, 4190.
- (14) Friedrichsen, W. *Adv. Heterocycl. Chem.* **1980**, *26*, 135.
- (15) Jacq, J.; Einhorn, C.; Einhorn, J. *Org. Lett.* **2008**, *10*, 3757.
- (16) Kiebooms, R. H. L.; Adriaenssens, P. J. A.; Vanderzande, D. J. M.; Gelan, J. M. J. V. *J. Org. Chem.* **1997**, *62*, 1473.
- (17) Hamura, T.; Nakayama, R. *Chem. Lett.* **2013**, *42*, 1013.
- (18) Sutton, C.; Marshall, M. S.; Sherrill, C. D.; Risko, C.; Bredas, J. L. *J. Am. Chem. Soc.* **2015**, *137*, 8775.
- (19) Paraskar, A. S.; Reddy, A. R.; Patra, A.; Wijsboom, Y. H.; Gidron, O.; Shimon, L. J. W.; Leitus, G.; Bendikov, M. *Chem. - Eur. J.* **2008**, *14*, 10639.
- (20) A single crystal of 2,8-difluoro-5,11-bis(4-fluorophenyl)-6,12-diphenyltetracene (F₄-RUB) has a packing motif similar to that of this crystal. See ref 21.
- (21) Braga, D.; Jaafari, A.; Miozzo, L.; Moret, M.; Rizzato, S.; Papagni, A.; Yassar, A. *Eur. J. Org. Chem.* **2011**, *2011*, 4160.
- (22) This polymorph is the same as crystal B reported by Zhang et al. in ref 11. They found three different crystals, A–C, all with twisted PF-RUB molecules.
- (23) The cell volumes for F₁₀-RUB and F₂₀-RUB crystals increased by 12.6% and 19.0% relative to that for RUB, respectively. See ref 12.
- (24) Meyer, E. A.; Castellano, R. K.; Diederich, F. *Angew. Chem., Int. Ed.* **2003**, *42*, 1210.
- (25) Swartz, C. R.; Parkin, S. R.; Bullock, J. E.; Anthony, J. E.; Mayer, A. C.; Malliaras, G. G. *Org. Lett.* **2005**, *7*, 3163.
- (26) Chen, Z. H.; Muller, P.; Swager, T. M. *Org. Lett.* **2006**, *8*, 273.
- (27) Very recently, Ogden et al. reported a similar 2D brick packing of F₁₀-RUB. Unlike F₁₄-RUB, it adopted an alternate arrangement in a 2D layer. See ref 12.
- (28) Akita, R.; Kawanishi, K.; Hamura, T. *Org. Lett.* **2015**, *17*, 3094.